Solute uptake through the walls of a pulsating channel

By S. L. WATERS†

Department of Applied Mathematics and Theoretical Physics,
University of Cambridge, Silver Street, Cambridge, CB3 9EW, UK

We investigate the uptake of a passive solute through the walls of a pulsating, fluid-filled channel into an adjacent medium in which the solute diffuses and is consumed at a constant rate. One end of the channel is open to well-mixed fluid containing the solute. The channel walls oscillate periodically in time and this prescribed motion generates steady streaming within the channel. We determine how this flow enhances the overall solute consumption (i.e. the flux of solute into the channel), the solute dispersion along the channel and the quantity of solute in the adjacent medium. The solute disperses in the channel due to the interaction between advection and transverse diffusion. The time-mean solute distribution throughout the channel and the medium is determined for a wide range of parameters. The results are applied to a new surgical technique used to treat patients with severe coronary artery disease, in which narrow tubes are created within ischemic heart muscle in an attempt to reperfuse the area directly with oxygenated blood.

1. Introduction

Transmyocardial laser revascularisation (TMLR) is used to treat patients with severe coronary artery disease. Although procedures such as coronary angioplasty and coronary artery bypass grafting are proven methods of treating heart disease, many patients have conditions that are not amenable to these therapies. TMLR was proposed as a means of bypassing the coronary circulation altogether, instead perfusing the myocardium (heart muscle) with oxygenated blood directly from the left-ventricular chamber, in a manner similar to embryonic and reptilian cardiac circulations. Using a laser (carbon dioxide or holmium), 10 to 50 narrow tunnels are drilled in the left-ventricular myocardium, which are closed at the epicardial surface and open to the left-ventricular cavity at the endocardial surface. The tunnels are typically ~ 1 mm in diameter and are created ~ 1 cm apart (Horvath *et al.* 1995).

Much controversy surrounds the efficacy of this procedure (Pretre & Turina 1999). The success of any type of myocardial revascularisation lies in the improvement in the delivery of oxygenated blood to the ischemic area, providing relief from angina. Although the exact mechanism of TMLR is unknown, improved perfusion and relief of symptoms after treatment could result from patent (open) tunnels created by the laser or from laser-induced angiogenesis. While some studies have found evidence of tunnel patency and of angiogenesis (Frazier, March & Horvath 1999 and references therein; Kadipasaoglu *et al.* 1997; Berwing *et al.* 1997) others have failed to find

† Present address: Division of Theoretical Mechanics, School of Mathematical Sciences, University of Nottingham, University Park, Nottingham, NG7 2RD, UK.

such evidence (Hardy *et al.* 1987; Landreneau *et al.* 1991; Mueller *et al.* 1998). Schofield *et al.* (1999) found no evidence of improved cardiac function or myocardial perfusion, although they did find that the treatment provided relief from angina symptoms. Critics of TMLR have suggested that the decrease in the severity of angina symptoms may be a placebo effect (Lange & Hillis 1999). The conflict in the results of the clinical studies may be due to the variety of experimental models and differences in the various physical parameters of the laser, such as its energy and pulse duration. If the treatment is to be effective in the future, it is necessary to determine the underlying mechanisms involved.

In the first few months after treatment, it is possible that blood flow through patent tunnels plays an important role in the efficacy of the treatment (Horvath *et al.* 1995). We hypothesize that this blood flow enhances the quantity of oxygenated blood drawn into the tunnel and the subsequent delivery of oxygen to the tissue. Since the tunnels are within the heart muscle, their overall geometry, represented by the tunnel diameter and length, changes with time as the heart beats. This tunnel wall motion will result in a fluid flow, the details of which depend on the precise nature of the wall motion and the tunnel geometry. The quantity and distribution of oxygen in the tunnel and its transport into the surrounding ischemic tissue will then be determined by its molecular diffusivity, the blood flow within the tunnel, the tunnel wall permeability and the rate of oxygen consumption within the tissue.

When a passive solute is injected into fluid flowing along a tube or channel, it spreads out along the tube in the direction of the flow owing to (i) longitudinal molecular diffusion and (ii) the interaction between advection and transverse diffusion. The dispersion of a bolus of diffusing solute in a fluid flowing along a long, rigid, cylindrical, impermeable tube was first studied by Taylor (1953) and Aris (1956), who generalized Taylor's results. Taylor showed that the longitudinal spreading of the solute is enhanced because of the non-uniform velocity profile and limited by lateral mixing.

Following Taylor's paper, a wide variety of dispersion problems has been analysed. Dispersion in a long, rigid, straight, impermeable tube or channel when the flow is driven by an oscillatory axial pressure gradient has been studied by Harris & Goren (1967), Chatwin (1975) and Watson (1983). Hydon & Pedley (1993) analysed solute transport through a fluid within a long, but finite, channel or pipe, whose impermeable walls remain parallel but oscillate transversely. These authors assumed that away from the ends of the channel the flow will be very closely approximated by the flow in an infinitely long, parallel-sided channel with identical transverse wall motion, as analysed by Secomb (1978). They calculated the axial dispersion of the solute over a wide parameter range and found the mean longitudinal transport to be greatly enhanced when the steady streaming Reynolds number (defined below) is much greater than unity.

Mass transfer between a flowing fluid and an adjacent stationary medium can greatly alter the overall solute dispersion. A number of workers have investigated the effect of boundary absorption or a catalytic wall reaction on shear dispersion (Purnama 1995; Mazumder & Das 1992; Phillips & Kaye 1998), but without considering the influence of solute consumption within the adjacent stationary medium.

To determine how the blood flow, driven by the wall motion of the laser-created tunnels, enhances the delivery of oxygen to the surrounding ischemic tissue, we develop the following idealized, two-dimensional model. The blood is assumed to be a homogeneous, incompressible, Newtonian fluid and the oxygen is modelled as a passive solute. The tissue is assumed to be a homogeneous medium in which the solute diffuses and is consumed at a constant rate. Since the tunnels are narrow

and spaced relatively far apart, we consider a single tunnel in a transversely infinite medium. The tunnel is modelled as a two-dimensional channel, which is long, but finite, and open at one end to well-mixed fluid containing the passive solute. The channel walls are permeable to the solute only. The fluid flow in the channel is governed by the continuity and the Navier–Stokes equations together with the no-slip boundary condition at the channel walls. The transport of solute is modelled by an advection–diffusion equation in the channel and a diffusion–consumption equation in the surrounding medium; these equations are coupled via the boundary conditions at the permeable channel walls. As a first step, we take the variation in channel half-width and length to be sinusoidal in time, with dimensionless frequency $\alpha \sim O(1)$ and asymptotically small amplitude ε. This choice of sinusoidal variation is motivated by the fact that both the channel length and half-width will increase as the heart expands and decrease as it contracts. By considering a parameter expansion in powers of ε for the dependent variables we are able to determine the fluid flow within the channel and the corresponding time-mean solute distribution within the channel and the medium. Since the molecular diffusivity of oxygen in blood is small, longitudinal diffusion is negligible and the dominant spreading mechanism for the solute in the channel is due to the interaction between advection and transverse diffusion (shear dispersion). The analysis will be restricted to the transport of solutes in liquids for which the Schmidt number, the ratio of kinematic viscosity to molecular diffusivity, is large. Note that the assumption of two-dimensionality is made because the analysis is simpler, and therefore the physical mechanisms more transparent, than in the corresponding axisymmetric model.

In §2 the problem is formulated mathematically and a similarity solution for the fluid flow within the channel is given. In §3 we derive the governing equations for the time-mean solute concentration and in §4 these equations are solved subject to the appropriate boundary conditions. Two particular cases are investigated in detail, corresponding to relatively small and to large channel-wall permeability. Finally in §5 we discuss the physiological implication of the results. We find that the fluid motion within the channel significantly enhances the delivery of solute to the medium. Thus the hypothesis of Horvath *et al.* (1995), that blood flow through patent tunnels may be important in the efficacy of the treatment, is likely to be true.

2. Formulation

We consider a two-dimensional, rigid channel surrounded by a homogeneous medium; see figure 1. A Cartesian coordinate system (x^*, y^*) is chosen with corresponding coordinate directions $(\hat{\boldsymbol{x}}, \hat{\boldsymbol{y}})$. Throughout this paper asterisks denote dimensional quantities. The channel is assumed to be closed at one end by an idealized compliant membrane, which prevents only axial motion, leaving motion in the $\hat{\boldsymbol{y}}$-direction completely unrestricted. This end corresponds to $x^* = 0$ and is assumed not to move in the axial direction. The channel length, $b^*(t^*)$, varies with time, t^*. The channel walls move along their normal direction (the $\hat{\boldsymbol{y}}$-direction) in a prescribed way, so that

$$y^* = a^*(t^*) \tag{2.1}$$

at the channel–medium interface. Here, a^* is the channel half-width. The variation of the channel half-width and length with time is assumed to be oscillatory so that

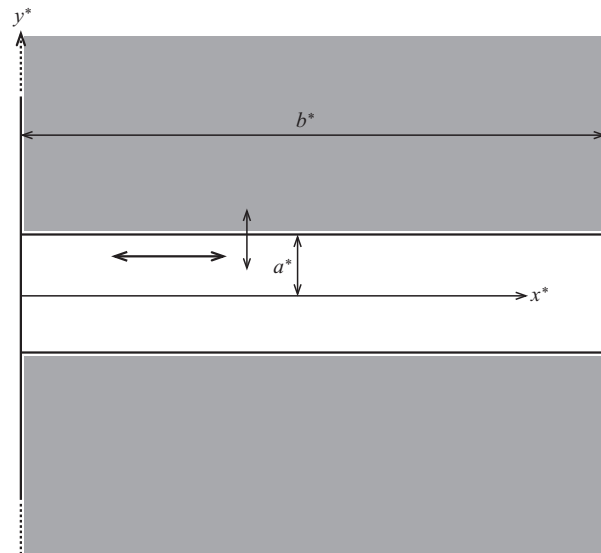$$(a^*, b^*) = (a_0^*, b_0^*)a \quad \text{where } a = (1 + \varepsilon \sin \omega^* t^*). \tag{2.2}$$

FIGURE 1. Definition sketch.

The time-mean half-width and length are a_0^*, b_0^* respectively, ε is the amplitude and ω^* is the angular frequency of the oscillations.

The channel contains a homogeneous, incompressible, Newtonian fluid, which has velocity components (u^*, v^*) and pressure p^*. The kinematic viscosity is denoted by v^* and ρ^* is the fluid density. The open end of the channel is exposed to well-mixed fluid containing solute at concentration C_0^* and the solute concentrations in the channel and the surrounding medium are $C_0^* C$ and $C_0^* \theta$ respectively. The solute diffusivity, D^*, is assumed to be the same in both the fluid and the medium since the tissue is predominantly composed of water. The medium consumes solute at a constant rate Q^*. The closed end of the channel is assumed to be impermeable to both fluid and solute. The interfacial wall is impermeable to fluid but allows the passage of solute with a permeability coefficient β^*.

2.1. Physiological parameter values

The following physiological parameter values are taken from the literature. The typical radius of the laser drilled holes is 0.5×10^{-3} m (Jansen *et al.* 1997) and so we take this to be the value of a_0^* in our two-dimensional model. The mean channel length $b_0^* \sim 1 \times 10^{-2}$ m and the angular frequency $\omega^* \sim 2\pi \, \mathrm{s}^{-1}$. The kinematic viscosity of blood $v^* \sim 4 \times 10^{-6} \, \mathrm{m}^2 \, \mathrm{s}^{-1}$ and the diffusivity of oxygen in blood $D^* \sim 2.4 \times 10^{-9} \, \mathrm{m}^2 \, \mathrm{s}^{-1}$ (Sharan, Aminataei & Singh 1987). The tissue is assumed to consume oxygen at a rate $Q^* C_0^* \theta$, where $Q^* \sim 2 \times 10^{-3} \, \mathrm{s}^{-2}$ (Salathé & Wang 1980) and the wall permeability coefficient, based on the permeability coefficient of capillaries, is $\beta^* \sim 2 - 50 \times 10^{-6} \, \mathrm{m} \, \mathrm{s}^{-2}$ (Salathé & Wang 1980). The value of β^* appropriate to the laser-drilled channels is expected to be greater than this. However, there is evidence that, after a period of about a month, the channels become lined with a layer of fibrin thrombus which might reduce the wall permeability (Horvath *et al.* 1995).

2.2. Fluid flow

The fluid flow is governed by the continuity and the Navier–Stokes equations. It is helpful to choose a frame of reference in which the channel walls are fixed and so,

following Secomb (1978), we non-dimensionalize as follows:

$$t^* = t/\omega^*, \quad x^* = b^*\xi, \quad y^* = a^*\eta, \quad u^* = \omega^* b_0^* u, \quad v^* = \omega^* a_0^* v, \quad p^* = \rho^* (b_0^* \omega^*)^2 p.$$

$$(2.3)$$

The dimensionless governing equations are
continuity:

$$\frac{\partial u}{\partial \xi} + \frac{\partial v}{\partial \eta} = 0, \tag{2.4a}$$

axial momentum:

$$\left(-\frac{\dot{a}}{a}\eta\frac{\partial}{\partial \eta} - \frac{\dot{a}}{a}\xi\frac{\partial}{\partial \xi} + \frac{\partial}{\partial t} \right)u + \frac{u}{a}\frac{\partial u}{\partial \xi} + \frac{v}{a}\frac{\partial u}{\partial \eta} = -\frac{1}{a}\frac{\partial p}{\partial \xi} + \frac{1}{\alpha^2 a^2}\left(\frac{\partial^2 u}{\partial \eta^2} + \delta^2 \frac{\partial^2 u}{\partial \xi^2} \right), \tag{2.4b}$$

transverse momentum:

$$\left(-\frac{\dot{a}}{a}\eta\frac{\partial}{\partial \eta} - \frac{\dot{a}}{a}\xi\frac{\partial}{\partial \xi} + \frac{\partial}{\partial t} \right)v + \frac{u}{a}\frac{\partial v}{\partial \xi} + \frac{v}{a}\frac{\partial v}{\partial \eta} = -\frac{1}{\delta^2 a}\frac{\partial p}{\partial \eta} + \frac{1}{\alpha^2 a^2}\left(\frac{\partial^2 v}{\partial \eta^2} + \delta^2 \frac{\partial^2 v}{\partial \xi^2} \right). \tag{2.4c}$$

The boundary conditions are

$$u = \dot{a}\xi, \quad v = \pm\dot{a} \quad \text{at } \eta = \pm1. \tag{2.5}$$

In the above equations, dots denote derivatives with respect to time. The two dimensionless parameters appearing in the governing equations for the fluid flow, in addition to ε which appears in $a(t)$, are the channel aspect ratio $\delta = a_0^*/b_0^*$ and the Womersley parameter $\alpha = a_0^*(\omega^*/v^*)^{1/2}$. Since we are considering a long, thin channel (corresponding to $\delta \ll 1$), we neglect terms of $O(\delta^2)$ in the governing equations for the flow and seek a similarity solution of the form

$$(u, v, p) = (a\xi U, aV, a^2\xi^2 P + P_0(\eta)), \tag{2.6}$$

where U, V and P are independent of ξ. Equation (2.4c) then shows that P is independent of η, and (2.4a) combines with (2.4b) to give a nonlinear equation for $V(\eta, t)$ which involves $P(t)$. Note that this similarity solution will not be valid at a dimensionless distance of $O(\delta)$ from the channel ends. The value of α based on the physiological parameter values given in §2.1 is ≈ 0.6 and so we take $\alpha = O(1)$.

The amplitude of the channel wall oscillations is assumed small and we consider a small-parameter expansion for the dependent variables in powers of ε (throughout this paper c.c. denotes complex conjugate):

$$U(\eta, t) = \varepsilon[U^{[11]}(\eta)e^{it} + \text{c.c.}] + \varepsilon^2[(U^{[20]}(\eta) + \text{c.c}) + (U^{[22]}(\eta)e^{2it} + \text{c.c.})] + \cdots, \tag{2.7}$$

with similar expansions for $V(\eta, t)$ and $P(t)$. The quantities $U^{[ij]}$ are independent of time and represent the jth Fourier coefficient of the ith-order term in the expansion of U. The time-independent terms of $O(\varepsilon^2)$ represent the steady streaming, which results from the convective inertia terms. Since the steady streaming Reynolds number, $R_s = \alpha^2\varepsilon^2$, is much less than unity we can carry out a uniform series expansion of the governing equations (2.4a)–(2.4c) by considering successive orders of ε. In order to determine the leading-order time-mean solute distribution we will require explicit expressions for $U^{[11]}, V^{[11]}$ and the axial steady streaming $U^{[20]}$. These are found to be

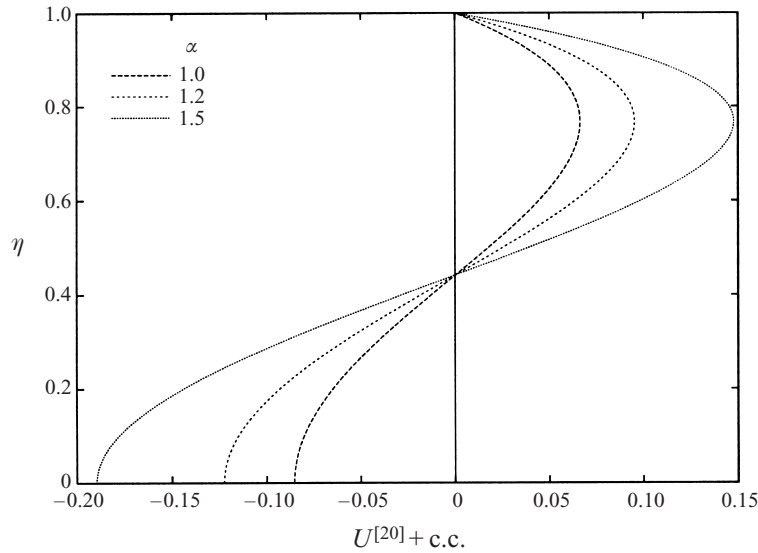$$U^{[11]} = \frac{1}{2E}\left[2\cosh k\eta - \cosh k - \frac{\sinh k}{k} \right], \tag{2.8a}$$

FIGURE 2. Axial steady streaming ($U^{[20]}$ + c.c.) for $\alpha = 1.0, 1.2, 1.5$. The channel wall is at $\eta = 1$ and the centreline at $\eta = 0$. The flow is towards $\xi = 1$ close to the channel walls and is towards $\xi = 0$ in the centre of the channel.

$$V^{[11]} = \frac{1}{2E} \left[-2\frac{\sinh k\eta}{k} + \eta \cosh k + \eta \frac{\sinh k}{k} \right], \quad (2.8b)$$

$$U^{[20]} = \frac{1}{EE'} \left\{ \tfrac{1}{2} \sinh k\eta \sinh k'\eta + \eta \sinh k\eta \sinh k' + 2\mathrm{i} \left[\cosh k' + \frac{\sinh k'}{k'} \right] \cosh k\eta \right.$$

$$\left. + \tfrac{3}{2} \sinh k'(\eta^2 - 1) \left[\frac{11}{2} \frac{\cosh k}{k} - \tfrac{3}{2} \sinh k \right] + \frac{2}{k} \sinh k' \cosh k - \tfrac{3}{2} \sinh k \sinh k' \right\},$$

$$(2.8c)$$

where $k = \alpha e^{\mathrm{i}\pi/4}$, $E = \cosh k - \sinh k/k$ and primes are used to denote the complex conjugate of a variable or parameter (see Secomb 1978). In figure 2 the axial steady streaming is plotted for three values of α. The flow is towards $\xi = 1$ close to the channel walls and is towards $\xi = 0$ in the centre of the channel.

3. Concentration equations and boundary conditions

The dimensionless governing equations for the solute concentration in the channel, C, and in the surrounding medium, θ, are respectively

$$\left(-\frac{\dot{a}}{a}\eta\frac{\partial}{\partial\eta} - \frac{\dot{a}}{a}\xi\frac{\partial}{\partial\xi} + \frac{\partial}{\partial t} \right) C + \xi U \frac{\partial C}{\partial\xi} + V \frac{\partial C}{\partial\eta} = \frac{1}{\sigma\alpha^2}\frac{1}{a^2}\left(\frac{\partial^2 C}{\partial\eta^2} + \delta^2\frac{\partial^2 C}{\partial\xi^2} \right), \quad (3.1a)$$

$$\left(-\frac{\dot{a}}{a}\eta\frac{\partial}{\partial\eta} - \frac{\dot{a}}{a}\xi\frac{\partial}{\partial\xi} + \frac{\partial}{\partial t} \right) \theta = \frac{1}{\sigma\alpha^2}\left\{ \frac{1}{a^2}\left(\frac{\partial^2\theta}{\partial\eta^2} + \delta^2\frac{\partial^2\theta}{\partial\xi^2} \right) - \lambda\theta \right\}, \quad (3.1b)$$

where $\sigma = v^*/D^*$ is the Schmidt number and $\lambda = a_0^{*2}Q^*/D^*$ is the ratio of the diffusion timescale to the consumption timescale in the medium. Based on the parameter values in §2.1 we have that $\sigma \sim 1.6 \times 10^3$ and $\lambda \sim 0.2$. The $O(\delta^2)$ terms in equations (3.1a)

and (3.1*b*) are neglected, as they are in equations (2.4); hence the effects of longitudinal diffusion are neglected here.

We shall determine the time-mean solute concentration in the channel and the surrounding medium. Consider the time average of equation (3.1*a*). Since the time-independent velocity is $O(\varepsilon^2)$ the ratio of the steady advection to the transverse molecular diffusion in (3.1*a*) is $O(\alpha^2 \sigma \varepsilon^2)$. We thus define the mean Péclet number, $\tilde{P}$, based on the channel half-width, to be

$$\tilde{P} = \alpha^2 \sigma \varepsilon^2. \tag{3.2}$$

Since the problem is symmetric about the channel centreline, we need only solve the problem in the upper half-η-plane. (Hall & Papageorgiou (1999) have found a rich set of asymmetric solutions to the flow problem, but these arise only if the Reynolds number exceeds a critical value, which depends on the dimensionless wall amplitude, and is outside our range of interest.) The boundary conditions for the solute concentration are

$$\frac{\kappa}{a} \frac{\partial C}{\partial \eta}\bigg|_{\eta=1} = -(C|_{\eta=1} - \theta|_{\eta=1}) = \frac{\kappa}{a} \frac{\partial \theta}{\partial \eta}\bigg|_{\eta=1}, \quad \frac{\partial C}{\partial \eta}\bigg|_{\eta=0} = 0, \quad \theta \to 0 \quad \text{as} \quad \eta \to \infty. \tag{3.3a–c}$$

The dimensionless parameter $\kappa = D^*/(a_0^* \beta^*)$ is the ratio of the timescales of uptake and diffusion and its value lies between $O(10^{-1})$ and $O(1)$. Condition (3.3*a*) describes continuity of solute flux at the channel–medium interface and allows jumps in the solute concentration. Equation (3.3*b*) is the zero-flux condition at the centre of the channel. Equation (3.3*c*) states that the solute concentration in the medium decays away from the channel walls in the transverse direction.

To determine the solute concentration completely, it is necessary to specify end boundary conditions at $\xi = 0$ and $\xi = 1$. We assume that there is no flux of solute through the walls at $\xi = 0$ so that

$$\left.\begin{array}{ll} \dfrac{\partial C}{\partial \xi} = 0 & \text{for } 0 \leqslant \eta \leqslant 1 \\[2mm] \dfrac{\partial \theta}{\partial \xi} = 0 & \text{for } \eta > 1 \end{array}\right\} \quad \text{at} \quad \xi = 0. \tag{3.4a, b}$$

The conditions at $\xi = 1$ are less straightforward. Much of the work on shear dispersion assumes that, when advection dominates longitudinal molecular diffusion, a one-dimensional advection–diffusion–reaction equation is valid far downstream from a change in conditions. Since this one-dimensional equation is far simpler than the corresponding full governing equations, it is natural to extend its use to the channel ends, although it is not a valid approximation there. However, by determining the appropriate boundary conditions at the channel ends it is possible to ensure that far downstream of a change in conditions the solutions of the one-dimensional equation are as close as possible to the solutions of the full equations. Smith (1988) considered the transport of a dilute reactive solute in a plane, steady, parallel flow in a flow reactor, when advection dominates molecular diffusion. In order to determine the appropriate boundary conditions for the one-dimensional model accurately, it was necessary to solve the full three-dimensional concentration equations.

In this problem, we do not determine the velocity profile at the channel entrance and so we cannot determine the full two-dimensional concentration profile in this region. Instead we impose a condition at the channel entrance that is independent of

η as follows. The ratio of steady advection to mean longitudinal diffusion is $O(\tilde{P}/\delta^2)$ so that the dominant mechanism for solute transport at the channel entrance is advection. We make the approximation that the concentration at $\xi = 1$ is given by $C = 1$. During inflow, the channel draws in well-mixed fluid and so this condition is accurate. During outflow, however, the fluid will leave the channel as a jet and the concentration of solute at the exit will thus be determined by the concentration in the fluid that was previously upstream. However, we assume that the error due to the imposed condition will be exponentially small outside a thin boundary layer (see Hydon 1991). As we will see below, it is not necessary to impose a boundary condition on the tissue concentration at $\xi = 1$. We impose that the solute concentration in the medium responds accordingly.

In §4 we shall determine how the fluid flow enhances the solute flux into the channel. The solute flux at the channel entrance, F^*, is given by

$$F^* = -2\int_0^{a^*} (u^*C^* - D^*C_{x^*}^*)\,\mathrm{d}y^*\big|_{x^*=b^*}$$

$$= -2\frac{C_0^* v^* b_0^*}{a_0^*}\alpha^2 \int_0^1 \left(a^2\xi UC - \frac{\delta^2}{\sigma\alpha^2}C_\xi\right)\mathrm{d}\eta\bigg|_{\xi=1}. \tag{3.5}$$

Since we are neglecting $O(\delta^2)$ terms, we have

$$\mathscr{S} = \frac{F^* a_0^*}{2C_0^* v^* b_0^*} = -\alpha^2 \int_0^1 a^2\xi UC\,\mathrm{d}\eta\big|_{\xi=1}, \tag{3.6}$$

where $\mathscr{S}$ is a measure of the effect of the fluid flow on the solute transport. The time-mean component of $\mathscr{S}$ is denoted by $\mathscr{S}_m$.

3.1. *Time-mean concentration equations*

To determine the leading-order time-mean governing equations for the solute concentrations in the channel and the medium we expand C and θ in powers of ε as follows:

$$C(\eta, \xi, t) = \mathscr{C}(\eta, \xi) + \varepsilon[C^{[11]}(\eta, \xi)\mathrm{e}^{it} + \text{c.c.}] + O(\varepsilon^2), \tag{3.7a}$$

$$\theta(\eta, \xi, t) = \Theta(\eta, \xi) + \varepsilon[\theta^{[11]}(\eta, \xi)\mathrm{e}^{it} + \text{c.c.}] + O(\varepsilon^2). \tag{3.7b}$$

We then consider equations (3.1*a*) and (3.1*b*) at various orders of ε. From equation (3.2) with $\alpha = O(1)$, we have $\sigma \sim O(\tilde{P}\varepsilon^{-2})$. Equation (3.1*a*) at $O(\varepsilon)$ gives

$$C^{[11]} = \mathrm{i}[-\tfrac{1}{2}\eta + V^{[11]}]\frac{\partial\mathscr{C}}{\partial\eta} + \mathrm{i}\xi[-\tfrac{1}{2} + U^{[11]}]\frac{\partial\mathscr{C}}{\partial\xi}. \tag{3.8}$$

This expression for $C^{[11]}$ is then substituted into equation (3.1*a*) at $O(\varepsilon^2)$, the time average is taken, and the following governing equation for $\mathscr{C}$ is obtained:

$$\xi\tilde{\mathscr{U}}\frac{\partial\mathscr{C}}{\partial\xi} + \tilde{\mathscr{V}}\frac{\partial\mathscr{C}}{\partial\eta} = \frac{1}{\tilde{P}}\frac{\partial^2\mathscr{C}}{\partial\eta^2}, \tag{3.9a}$$

where $\tilde{\mathscr{U}} = U^{[20]} - \mathrm{i}U_\eta^{[11]'}(-\eta/2 + V^{[11]}) + \text{c.c.}$ and $\tilde{\mathscr{V}} = V^{[20]} + \mathrm{i}(1/2 - V_\eta^{[11]'})(-\eta/2 + V^{[11]}) + \text{c.c.}$ In order that the radial diffusion term enters the governing equation at this order we suppose that $\varepsilon \ll \tilde{P} \ll \varepsilon^{-1}$.

From equation (3.1*b*) we obtain the following equation for Θ:

$$\frac{\partial^2 \Theta}{\partial \eta^2} - \lambda \Theta = 0, \tag{3.9b}$$

which has solution

$$\Theta = A(\xi) \exp(-\lambda^{1/2} \eta), \tag{3.10}$$

where $A(\xi)$ is determined from the interfacial boundary condition (3.3*a*) and depends on $\mathscr{C}$.

We now proceed to solve (3.9*a*) for $\mathscr{C}$ subject to the boundary conditions (3.3*a*, *b*), (3.4*a*) and the condition $\tilde{\mathscr{C}} = 1$ at $\xi = 1$. Significant analytical progress may be made by assuming that $\tilde{P}$ is much less than 1. Thus we consider the asymptotic regime corresponding to $\varepsilon \ll \tilde{P} \ll 1$ so that the Schmidt number is in the range $\varepsilon^{-1} \ll \sigma \ll \varepsilon^{-3}$. This requirement of large Schmidt number is consistent with the value of the Schmidt number estimated for oxygen in blood; see §2.1.

3.2. *Cross-sectional averaging*

When $\tilde{P} \ll 1$, cross-channel diffusion dominates and acts to equilibrate the concentration of solute across the channel so that $\mathscr{C}$ may be decomposed into a component independent of η and a small fluctuation:

$$\mathscr{C} = \hat{\mathscr{C}}(\xi) + \tilde{P} \mathscr{C}^{(1)}(\xi, \eta), \tag{3.11}$$

where, for any f, $\hat{f} = \int_0^1 f \, \mathrm{d}\eta$ and $\widehat{\mathscr{C}^{(1)}} \equiv 0$ by definition ($\tilde{P} \mathscr{C}^{(1)}$ here includes terms of all orders $\geqslant 1$ in $\tilde{P}$). Substitution of (3.11) into (3.9*a*) gives

$$\xi \tilde{\mathscr{U}} \left(\frac{\partial \hat{\mathscr{C}}}{\partial \xi} + \tilde{P} \frac{\partial \mathscr{C}^{(1)}}{\partial \xi} \right) + \tilde{P} \tilde{\mathscr{V}} \frac{\partial \mathscr{C}^{(1)}}{\partial \eta} = \frac{\partial^2 \mathscr{C}^{(1)}}{\partial \eta^2}. \tag{3.12}$$

Integration of (3.12) with respect to η between 0 and 1 gives

$$\tilde{P} \xi \widehat{\tilde{\mathscr{U}} \mathscr{C}^{(1)}_\xi} + \tilde{P} \widehat{\tilde{\mathscr{V}} \mathscr{C}^{(1)}_\eta} = \left. \frac{\partial \mathscr{C}^{(1)}}{\partial \eta} \right|_{\eta=1}, \tag{3.13}$$

where the terms on the left-hand side represent the effects of shear dispersion. To determine the governing equation for $\hat{\mathscr{C}}$ it is necessary to compute the concentration fluctuation, $\mathscr{C}^{(1)}$, which is found by considering the $O(1)$ terms in equation (3.12):

$$\mathscr{C}^{(1)} = \xi \frac{\partial \hat{\mathscr{C}}}{\partial \xi} \int^\eta \mathscr{F} \, \mathrm{d}\eta \quad \text{where } \mathscr{F} = \int_0^\eta \tilde{\mathscr{U}} \, \mathrm{d}\eta. \tag{3.14}$$

We also require $\partial \mathscr{C}^{(1)} / \partial \eta$ at $\eta = 1$, which is, from the interfacial boundary condition (3.3*a*) and to leading order in ε,

$$\left. \frac{\partial \mathscr{C}^{(1)}}{\partial \eta} \right|_{\eta=1} = -\frac{\Delta}{\tilde{P}} \hat{\mathscr{C}} \quad \text{where } \Delta = \frac{\lambda^{1/2}}{1 + \kappa \lambda^{1/2}}. \tag{3.15}$$

Substitution of expressions (3.14) and (3.15) into equation (3.13) gives the following

ordinary differential equation in ξ for $\hat{\mathscr{C}}$:

$$\xi^2 \frac{\partial^2 \hat{\mathscr{C}}}{\partial \xi^2} + 2\xi \frac{\partial \hat{\mathscr{C}}}{\partial \xi} - \gamma \hat{\mathscr{C}} = 0, \quad \text{where} \quad \gamma = \frac{\Delta}{\tilde{P}^2} \frac{1}{\displaystyle\int_0^1 \mathscr{F}^2 \, d\eta}. \tag{3.16}$$

Physically, γ is a measure of the degree of solute uptake relative to dispersion.

Note that the solution for $\hat{\mathscr{C}}$ will not be valid at distances of $O(\tilde{P})$ from the channel entrance since in this region the axial advection term in equation (3.9a) is the same order as the transverse diffusion term. There, transverse diffusion does not dominate and equilibrate the concentration of solute across the channel so the decomposition for $\mathscr{C}$ given by equation (3.11) is not valid in that region.

4. Results

It is straightforward to solve equation (3.16) and the form of the solution depends on γ. For asymptotically small solute uptake, corresponding to $\gamma \ll 1$, the trivial solution is that $\hat{\mathscr{C}} = 1$ to leading order. Thus in the limit $\gamma \to 0$ the solution for an impermeable channel is recovered. For $\gamma = O(1)$ the dependence of $\hat{\mathscr{C}}$ on ξ is algebraic and the algebraic exponent is the positive root, m_1, of $m^2 + m - \gamma = 0$ (in order that the end boundary condition at $\xi = 0$ be satisfied it is also necessary that $m_1 > 1$, i.e. $\gamma > 2$). The most physiologically realistic limit, however, corresponds to $\gamma \gg 1$ and it is this limit that we consider in detail here.

When $\gamma \gg 1$, we have that $\hat{\mathscr{C}} \equiv 0$ except at small distances from the channel entrance. To determine the solute distribution in this region we introduce a stretched coordinate, $\hat{X}$, such that $1 - \xi = \hat{X}\gamma^{-1/2}$. Since we are considering distances greater than $O(\tilde{P})$ from the channel entrance, we require $\tilde{P} \ll \gamma^{-1/2} \ll 1$, which corresponds to $\Delta^{1/2} \ll 1$.

Equation (3.16) then reduces, at leading order, to $\hat{\mathscr{C}}_{\hat{X}\hat{X}} - \hat{\mathscr{C}} = 0$, the solution of which, satisfying $\hat{\mathscr{C}}(1) = 1$ and $\hat{\mathscr{C}}(\infty) = 0$ is $\hat{\mathscr{C}} = e^{-X}$, so in original variables

$$\hat{\mathscr{C}} = \exp\left\{ -\frac{1}{\tilde{P}} \frac{1}{\sqrt{\displaystyle\int_0^1 \mathscr{F}^2 \, d\eta}} \sqrt{\frac{\lambda^{1/2}}{1 + \kappa\lambda^{1/2}}} (1 - \xi) \right\}. \tag{4.1a}$$

From (3.11) together with boundary condition (3.3a), the leading-order concentration in the medium is

$$\Theta = \frac{1}{1 + \kappa\lambda^{1/2}} \hat{\mathscr{C}} \exp\left\{ \lambda^{1/2}(1 - \eta) \right\}. \tag{4.1b}$$

To determine how the solute flux entering the channel, the solute dispersion along the channel and the solute concentration in the medium depend on the governing parameters, we consider two limiting cases: $\kappa \gg 1$, $\lambda = O(1)$ and $\kappa = O(1)$, $\lambda \ll 1$, which correspond to relatively small and to large wall permeability respectively.

4.1. Small wall permeability

When $\kappa \gg 1$ and $\lambda = O(1)$, the leading-order expressions for the time-mean component of the solute flux at the channel entrance, $\mathscr{S}_m$, and the solute concentrations in

the channel and the medium are respectively

$$\mathscr{S}_m = \frac{1}{\sigma\kappa} \frac{\int_0^1 \left(\frac{\mathrm{i}}{2} V^{[11]'} \mathscr{F} + \text{c.c.} \right) \mathrm{d}\eta}{\sqrt{\int_0^1 \mathscr{F}^2 \, \mathrm{d}\eta}}, \tag{4.2a}$$

$$\hat{\mathscr{C}} = \exp\left\{ -\frac{1}{\sigma\epsilon^2\kappa^{1/2}} \frac{1}{\alpha^2 \sqrt{\int_0^1 \mathscr{F}^2 \mathrm{d}\eta}} (1 - \xi) \right\}, \tag{4.2b}$$

$$\Theta = \frac{1}{\kappa\lambda^{1/2}} \hat{\mathscr{C}} \exp\left\{ \lambda^{1/2}(1 - \eta) \right\}. \tag{4.2c}$$

From (4.2c), the medium concentration is an $O(1/\kappa)$ quantity and decays over an $O(1)$ lengthscale in the transverse direction (since $\lambda = O(1)$). Thus in this regime, corresponding to relatively small wall permeability, the quantity of solute reaching the medium is asymptotically small. From (4.2b), we note also that $\hat{\mathscr{C}}$ does not depend on λ and hence does not depend on the consumption, Q^*, since the wall permeability is sufficiently small that the solute concentration in the channel does not respond to variations in the solute consumption in the medium. Moreover, $\mathscr{S}_m$ does not depend on Q^*, but rather is limited by the permeability, β^*.

Next we investigate how the quantity of solute entering the channel varies with the governing parameters. In figure 3(a), $\mathscr{S}_m$ is plotted as a function of β^* for several values of α. As α increases, $\mathscr{S}_m$ increases as more solute is drawn into the channel by the fluid flow. Since $\sigma\kappa$ does not depend on the diffusivity, D^*, we see that $\mathscr{S}_m$ is independent of D^*. Increasing the permeability, β^*, results in $\mathscr{S}_m$ increasing. Solute is drawn into the channel during inflow and as β^* increases more of the solute is taken up by the medium. Thus, less solute is available to be expelled during outflow so that the time-mean solute flux into the channel increases.

The degree of dispersion of solute along the channel depends on the frequency parameter, α, and in figure 3(b), $\hat{\mathscr{C}}$ is plotted against ξ for several values of α ($\kappa = 0.5$, $\sigma = 10^3$, $\epsilon = 10^{-2}$). The concentration of solute at a given ξ increases as α increases, corresponding to the increase in the solute flux with α, and the solute penetrates further into the channel, due to the increased effects of shear dispersion. Since $\sigma \propto 1/D^*$ and $\kappa \propto D^*$, we see from (4.2b) that the solute concentration in the channel depends on $\sqrt{D^*}$. Increasing the diffusivity, D^*, causes $\hat{\mathscr{C}}$, at a given ξ, to decrease; see figure 4, where $\hat{\mathscr{C}}$ is plotted against ξ for several values of D^*. It can clearly be seen that the solute penetration into the channel decreases as D^* increases. As D^* increases, the fluctuations in the solute concentration across the cross-section are smaller (as diffusion more rapidly equilibrates the concentration) and the effects of shear dispersion are reduced. Finally, from (4.2b) we see that, since $\kappa \propto 1/\beta^*$, increasing β^* results in $\hat{\mathscr{C}}$ decaying more rapidly in the longitudinal direction so that the solute does not penetrate as far into the channel. Boundary uptake causes a depletion of solute in the channel and since the boundary tends to be the region of highest shear, the remaining solute experiences, on average, a reduced rate of shear dispersion (Smith 1983).
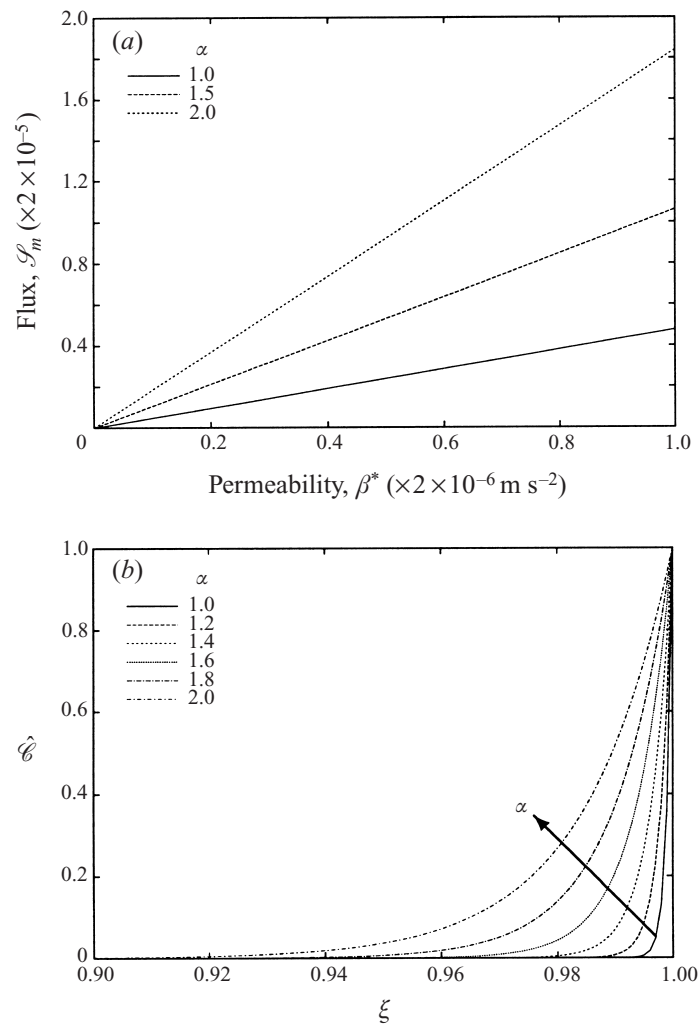
FIGURE 3. (a) Solute flux, $\mathcal{S}_m$, versus wall permeability, β^*, for several values of α. $\mathcal{S}_m$ increases with β^* and α. ($a_0^* = 10^{-3}$ m, $v^* = 10^{-6}$ m^2 s^{-1}.) (b) Solute concentration in the channel, $\hat{\mathcal{C}}$, versus ξ for several values of α. $\hat{\mathcal{C}}$ at a given ξ increases as α increases. ($\kappa = 0.5$, $\sigma = 10^3$, $\varepsilon = 10^{-2}$.)

Since $\Theta \propto \hat{\mathcal{C}}$, the quantity of solute reaching the medium is enhanced as α increases. The medium concentration, at any point, decreases with increasing D^*, but the lengthscale in the transverse direction over which it decays increases (since $\lambda \propto 1/D^*$). Essentially, increasing the diffusivity means that the solute spreads over a wider region in the medium. To determine how the medium concentration varies with β^*, we consider, for convenience, the medium concentration at $\eta = 1$. Increasing β^* causes the concentration to decay more rapidly in the axial direction (since $\Theta \propto \mathcal{C}$), but also results in an increase in the magnitude of Θ; see figure 5(a), where $\Theta|_{\eta=1}$ is plotted versus ξ for several values of β^*. Thus, near the channel entrance, Θ increases as β^* increases, but further into the channel the opposite is true. Increasing Q^* causes the solute concentration in the medium to decrease and to decay more rapidly in the transverse direction, as expected.
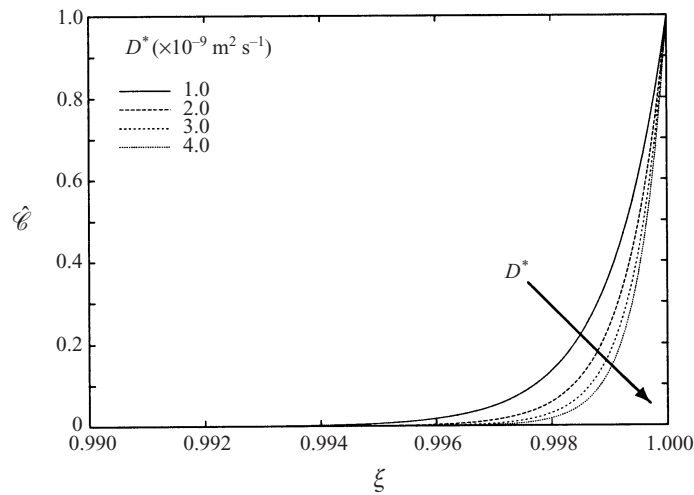
FIGURE 4. Solute concentration in the channel, $\hat{\mathscr{C}}$, versus ξ for various diffusivity, D^*. Channel concentration at a given ξ decreases as D^* increases. ($\alpha = 1$, $\nu^* = 10^{-6}\,\mathrm{m^2\,s^{-1}}$, $a_0^* = 10^{-3}\,\mathrm{m}$, $\beta^* = 2 \times 10^{-6}\,\mathrm{m\,s^{-2}}$, $\varepsilon = 10^{-2}$.)

4.2. *Large wall permeability*

In the limit of large wall permeability, corresponding to $\kappa = O(1)$ and $\lambda \ll 1$, we have

$$\mathscr{S}_m = \lambda^{1/2} \frac{\displaystyle\int_0^1 \left(\frac{\mathrm{i}}{2} V^{[11]'}\mathscr{F} + \text{c.c.}\right) \mathrm{d}\eta}{\sqrt{\displaystyle\int_0^1 \mathscr{F}^2 \, \mathrm{d}\eta}}, \tag{4.3a}$$

$$\hat{\mathscr{C}} = \exp\left\{-\frac{\lambda^{1/4}}{\sigma\epsilon^2} \frac{1}{\alpha^2 \sqrt{\displaystyle\int_0^1 \mathscr{F}^2 \, \mathrm{d}\eta}}(1 - \xi)\right\}, \tag{4.3b}$$

$$\Theta = \hat{\mathscr{C}} \exp\left\{\lambda^{1/2}(1 - \eta)\right\}. \tag{4.3c}$$

The functional dependence of $\mathscr{S}_m$, $\hat{\mathscr{C}}$ and Θ on α is as in §4.1. However, in contrast to §4.1, here the medium concentration is $O(1)$ over an $O(\lambda^{1/2})$ lengthscale in the transverse direction. Moreover, $\mathscr{S}_m$, $\hat{\mathscr{C}}$ and Θ are independent of the permeability, β^*, in this regime, i.e. the permeability is sufficiently large that it is no longer a limiting factor.

Since the wall permeability is now relatively much larger, the channel concentration is able to respond to variations in Q^* in the medium and we see that the time-mean solute flux, $\mathscr{S}_m$, and the solute concentration in the channel, $\hat{\mathscr{C}}$, depend on the solute consumption, Q^*, in the medium. As Q^* increases so too does $\mathscr{S}_m$ as more of the solute entering the channel during inflow is consumed in the medium so that less is expelled during outflow. The quantity of solute in the channel and the degree of penetration into the channel both decrease as Q^* increases; see figure 5(*b*) where $\hat{\mathscr{C}}$ is plotted against ξ for several values of Q^*. Increasing Q^* results in the channel concentration
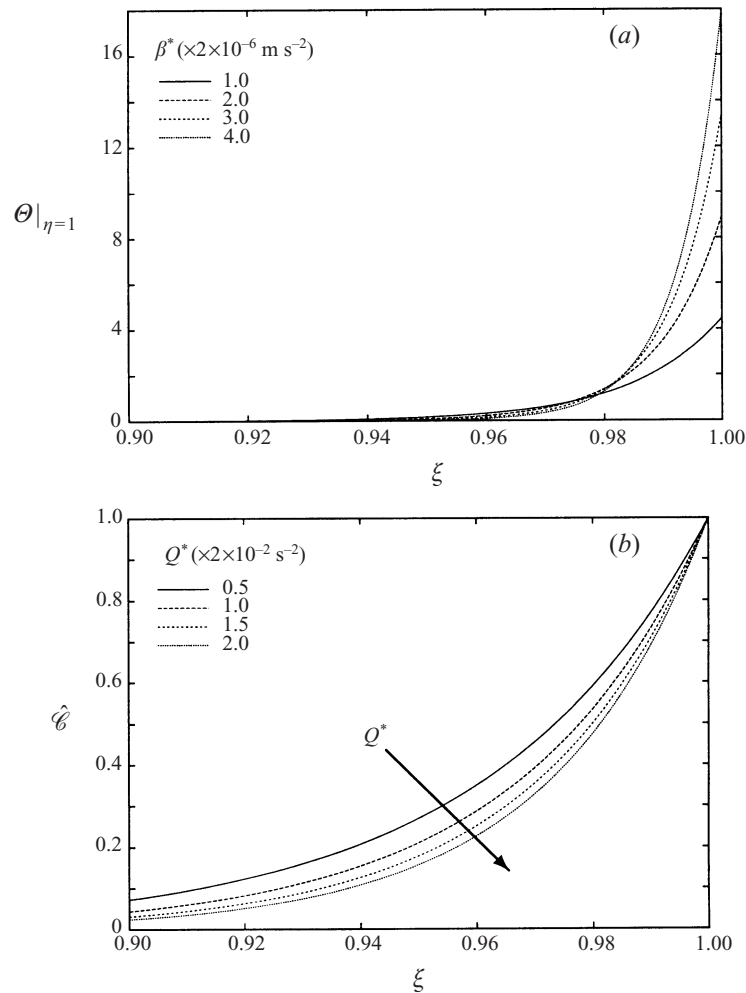
FIGURE 5. (a) Medium concentration at the interface, $\Theta|_{\eta=1}$, versus ξ for several values of the wall permeability, β^*. ($\sigma = 10^3$, $\lambda = 0.2$, $\alpha = 2$, $D^* = 10^{-9}\,\mathrm{m}^2\,\mathrm{s}^{-1}$, $a_0^* = 10^{-3}\,\mathrm{m}$.) (b) Solute concentration in the channel, $\hat{\mathscr{C}}$, versus ξ for several values of the solute consumption, Q^*. $\hat{\mathscr{C}}$ at a given ξ decreases as Q^* increases. ($\kappa = 0.5$, $\sigma = 10^3$, $\varepsilon = 10^{-2}$, $\alpha = 2$, $a_0^* = 10^{-3}\,\mathrm{m}$, $D^* = 10^{-9}\,\mathrm{m}^2\,\mathrm{s}^{-1}$.)

fluctuation decreasing so that the effects of shear dispersion are reduced. As before, increasing Q^* results in the solute concentration in the medium decreasing.

5. Conclusion and physiological applicability

We have shown that the steady streaming generated by the pulsations of a finite-length channel enhances the flux of solute into the open end of the channel, the dispersion of solute along the channel and the corresponding solute concentration in the surrounding medium. The solute disperses along the channel due to the interaction between advection and transverse diffusion. This mechanism becomes more effective as the molecular diffusivity decreases, since the channel concentration fluctuation is then relatively larger, and shear dispersion is more effective.

We considered in detail two limiting cases. In the first, corresponding to relatively

small wall permeability, the medium concentration is found to be asymptotically small. The wall permeability is a limiting factor in this regime and the solute consumption in the medium has no effect on the solute dispersion in the channel or the solute flux entering the channel. In the second regime, corresponding to large wall permeability, the medium concentration is $O(1)$ so that the delivery of solute to the medium is more effective. The wall permeability is no longer a limiting factor and so the solute consumption in the medium now impinges on the solute flux entering the channel and the solute dispersion in the channel. In particular, increasing the solute consumption causes the longitudinal dispersion of solute in the channel to decrease.

Physiologically, the second regime is the most interesting. We estimate that κ lies between $O(10^{-1})$ and $O(1)$. However, these values for κ are based on the permeability coefficient for capillaries and we might expect the walls of the laser-created channels to be more permeable than capillary walls so that the value of κ appropriate to the laser-drilled tunnels is smaller. We also estimate $\lambda = O(10^{-1})$ and hence the limit $\kappa = O(1)$, $\lambda \ll 1$ is the most appropriate. The concentration of solute in the medium is then an $O(1)$ quantity and increasing the frequency of the channel pulsations enhances the quantity of solute delivered to the medium. From (4.3a), we find that when $\alpha = 1$, $\mathscr{S}_m \approx 0.0048\lambda^{1/2}$, and when $\alpha = 2$, $\mathscr{S}_m \approx 0.018\lambda^{1/2}$ so that doubling the frequency of the oscillations leads to the quantity of solute reaching the tissue increasing by a factor of four. Care must be taken when extrapolating the results of our two-dimensional model to draw conclusions about the delivery of oxygen to the heart tissue via the laser-drilled channels. However, the results of our model indicate that the blood flow within the channel, generated by the channel wall motion, may be important in the efficacy of TMLR.

REFERENCES

ARIS, R. 1956 On the dispersion of a solute in a fluid flowing through a tube. *Proc. R. Soc. Lond.* A **235**, 67–77.

BERWING, K., BAUER, E. P., STRASSER, R., KLOVEKORN, W. P., REUTHEBUCH, O. & BERTSCHMANN, W. 1997 Functional evidence of long-term channel patency after transmyocardial laser revascularisation. *Circulation* **96** (Suppl.), 3156.

CHATWIN, P. C. 1975 On the longitudinal dispersion of passive contaminant in oscillatory flows in tubes. *J. Fluid Mech.* **71**, 513–527.

FRAZIER, O. H., MARCH, R. J. & HORVATH, K. A. 1999 Transmyocardial revascularisation with a carbon dioxide laser in patients with end-stage coronary artery disease. *New Engl. J. Med.* **341**, 1021–1028.

HALL, P. & PAPAGEORGIOU, D. T. 1999 The onset of chaos in a class of Navier–Stokes solutions. *J. Fluid Mech.* **393**, 59–87.

HARDY, R. I., BOVE, K. E., JAMES, F. W., KAPLAN, S. & GOLDMAN, L. 1987 A histologic study of laser-induced transmyocardial channels. *Lasers Surg. Med.* **6**, 563–573.

HARRIS, H. G. & GOREN, S. L. 1967 Axial diffusion in a cylinder with pulsed flow. *Chem. Engng Sci.* **22**, 1571–1576.

HORVATH, K. A., SMITH, W. J., LAURENCE, R. G., SCHOEN, F. J., APPLEYARD, R. F. & COHN,

L. H. 1995 Recovery and viability of an acute myocardial infarct after transmyocardial laser revascularisation. *J. Am. Coll. Cardiol.* **25**(1), 258–263.

HYDON, P. E. 1991 Modelling the pulmonary circulation and gas transport in the lung. PhD thesis, University of Cambridge.

HYDON, P. E. & PEDLEY, T. J. 1993 Axial dispersion in a channel with oscillating walls. *J. Fluid Mech.* **249**, 535–555.

JANSEN, E. D., FRENZ, M., KADIPASAOGLU, K. A., PFEFER, T. J., ALTERMATT, H. J., MOTAMEDI, M. & WELCH, A. J. 1997 Laser-tissue interaction during Transmyocardial Laser Revascularisation. *Ann. Thorac. Surg.* **63**, 640–7.

KADIPASAOGLU, K. A., PEHLIVANOGLU, S., CONGER, J. L., SASAKI, E., DE VILLALOBOS, D. H., CLOY, M., PILUIKO, V., CLUBB, F. J., COOLEY, D. A. & FRAZIER, O. H. 1997 Long- and short-term effects of transmyocardial laser revascularization in acute myocardial ischemia. *Lasers Surg. Med.* **20**, 6–14.

LANDRENEAU, R., NAWARAWONG, W., LAUGHLIN, H., RIPPERGER, J., BROWN, O., McDANIEL, W., McKOWN, D. & CURTIS, J. 1991 Direct CO_2 laser-induced revascularisation of the myocardium. *Lasers Surg. Med.* **11**, 35–42.

LANGE, R. A. & HILLIS, L. D. 1999 Transmyocardial laser revascularisation. *New Engl. J. Med.* **341**, 1075–1076.

MAZUMDER, B. S. & DAS, S. K. 1992 Effect of boundary reaction on solute dispersion in pulsatile flow through a tube. *J. Fluid Mech.* **239**, 523–549.

MUELLER, X. M., TEVAEARAI, H. H., GENTON, C. Y., BETTEX, D. & VON SEGESSER, L. K. 1998 Transmyocardial laser revascularisation in acutely ischaemic myocardium. *Eur. J. Cardiothorar. Surg.* **13**, 170–05.

PHILLIPS, C. G. & KAYE, S. R. 1998 Approximate solutions for developing shear dispersion with exchange between phases. *J. Fluid Mech.* **374**, 195–219.

PRETRE, P. & TURINA, M. I. 1999 Laser to the heart: magic but costly, or only costly? *Lancet.* **353**, 512–513.

PURNAMA, A. 1995 The dispersion of chemically active solutes in parallel flow. *J. Fluid Mech.* **290**, 263–277.

SALATHE, E. P. & WANG, T. C. 1980 Substrate concentrations in tissue surrounding single capillaries. *Math. Biosci.* **49**, 235–247.

SCHOFIELD, P. M., SHARPLES, L. D., CAINE, N., BURNS, S., TAIT, S., WISTOW, T., BUXTON, M. & WALLWORK, J. 1999 Transmyocardial laser revascularisation in patients with refractory angina: a randomised controlled trial. *Lancet* **353**, 519–524.

SECOMB, T. W. 1978 Flow in a channel with pulsating walls. *J. Fluid Mech.* **88**, 273–288.

SHARAN, M., AMINATAEI, A. & SINGH, M. P. 1987 A numerical study of the unsteady transport of gases in the pulmonary capillaries. *J. Math. Biol.* **25**, 433–452.

SMITH, R. 1983 Effect of boundary absorption upon longitudinal dispersion in shear flows. *J. Fluid Mech.* **134**, 161–177.

SMITH, R. 1988 Entry and exit conditions for flow reactors. *IMA J. Appl. Maths* **41**, 1–20.

TAYLOR, G. I. 1953 Dispersion of soluble matter in solvent flowing slowly through a tube. *Proc. R. Soc. Lond.* A **219**, 186–203.

WATSON, E. J. 1983 Diffusion in oscillatory pipe flow. *J. Fluid Mech.* **133**, 233–244.